N.F.H. Bright

CANADA

DEPARTMENT OF MINES AND TECHNICAL SURVEYS

MINES BRANCH

OTTAWA

MINERAL SCIENCES DIVISION

REPORT MS-65-13

Fe-Nb-OXIDES: PHASE RELATIONSHIPS AT 1180°C

by

A.C. Turnock

Physical Chemistry Section

Crown Copyright Reserved

February 1st, 1965

Paper prepared for submission for publication in the Journal of the American Ceramic Society

Mineral Sciences Division Report MS-65-13

Fe-Nb-OXIDES: PHASE RELATIONSHIPS AT 1180°C

by

A.C. Turnock*

- - - -

ABSTRACT

Subsolidus phase relationships of the oxides in the system Fe-Nb-O have been experimentally determined at 1180°C, 1 atm. total pressure, and variable partial pressures of oxygen.

Niobium pentoxide reacts readily with either ferrous or ferric oxide at subsolidus temperatures, and the following ternary compounds have been synthesized: $Fe_4Nb_2O_9$, $FeNbO_4$ and $FeNb_2O_6$. Also, it has been shown that the rutile structure of NbO_2 will take $FeNb_2O_6$ into solid solution, and that the spinel structure of Fe_3O_4 will incorporate up to 7 atomic % Nb.

---

*Senior Scientific Officer, Physical Chemistry Section, Mineral Sciences Division, Mines Branch, Department of Mines and Technical Surveys, Ottawa, Canada. Crown Copyright Reserved.

INTRODUCTION

Recent studies of the tantalates wodginite[1] and ixiolite[2] have focussed attention on the phase relationships in systems containing the oxides of Ta, Nb, Fe, Mn, and Sn. In a previous similar study of the system Fe-Ta-O[3], the oxidation and reduction behaviours of $FeTa_2O_6$ (tapiolite) and of $FeTaO_4$ were investigated. The analogous niobian compounds $FeNb_2O_6$ (columbite) and $FeNbO_4$ behave in a similar manner.

Also of interest is the incorporation of niobium into the spinel structure of Fe_3O_4, which may have applications in ferrite technology. These niobian magnetites are analogous to the tantalian magnetites except they do not have as large a range of non-stoichiometry.

EXPERIMENTAL PROCEDURE

Desired compositions were prepared from reagent grade chemicals. Fansteel Nb_2O_5 and Fisher C.R. Fe_2O_3 were used. The methods of mixing, firing, oxygen partial-pressure control, quenching and examination of the products have been reported previously[3].

PHASE RELATIONSHIPS

Reactions at 1180°C between the solid phases and oxygen at various partial pressures are listed in Table 1. The temperature of some preliminary runs was 1200°C, but this was found to be above the solidus and the lower temperature was consequently chosen for the sub-solidus study. The liquid phase, whose composition is within the triangle

Fe-FeO-$Fe_4Nb_2O_9$, quenched to a black, opaque glass. It attacked the Pt foil crucible, with resultant weight changes that prevented any accounting of oxygen movement in the charge.

Some of the data from Table 1 are plotted in Figure 1 to illustrate the changes of stable assemblages caused by variation of the partial pressure of oxygen. The data points show the bulk compositions of the products; their positions are plotted using the Fe:Nb ratios and the oxygen contents; both items as listed in Table 1. The scatter of points from the tie-lines indicates the accuracy of the experimental method.

The data are summarized by projecting the tie-lines for all values of oxygen pressure on to the composition plane to produce the phase diagram shown in Figure 2. It is an isothermal, polybaric (defining oxygen pressure as the pressure variable) projection. The oxidation or reduction reactions that limit the stability of the phases appear as 3-solid-phase triangles that are numbered and listed in Table II along with the values for their univariant oxygen pressure.

DESCRIPTION OF THE COMPOUNDS

In this paper, the phases are abbreviated as follows:

α-Nb_2O_5 = A,	Nb_2O_4 = D,	Fe_2O_3 = H,
Fe_3O_4 = M,	$Fe_4Nb_2O_9$ = S,	$FeNb_2O_6$ = T,
$FeNbO_4$ = U,	$Fe_{1-x}O$ = W.	

These letter designations also include ternary solid solutions of the phases in Figure 1.

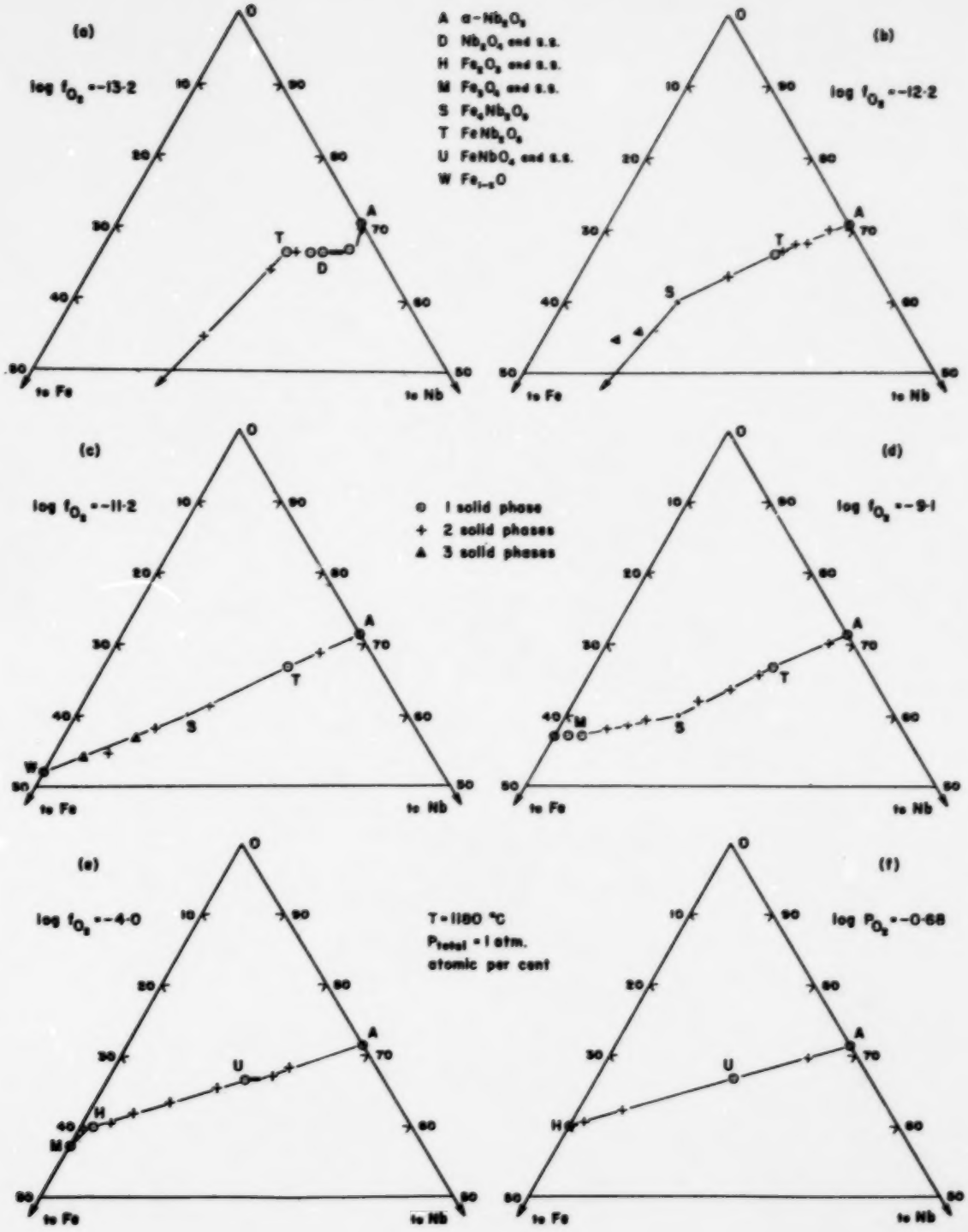

Figure 1. Isothermal, isobaric sections of the system Fe-Nb-O. Oxygen partial pressures as marked. Total pressure = 1 atm. Data from Table 1. s.s. = solid solution.

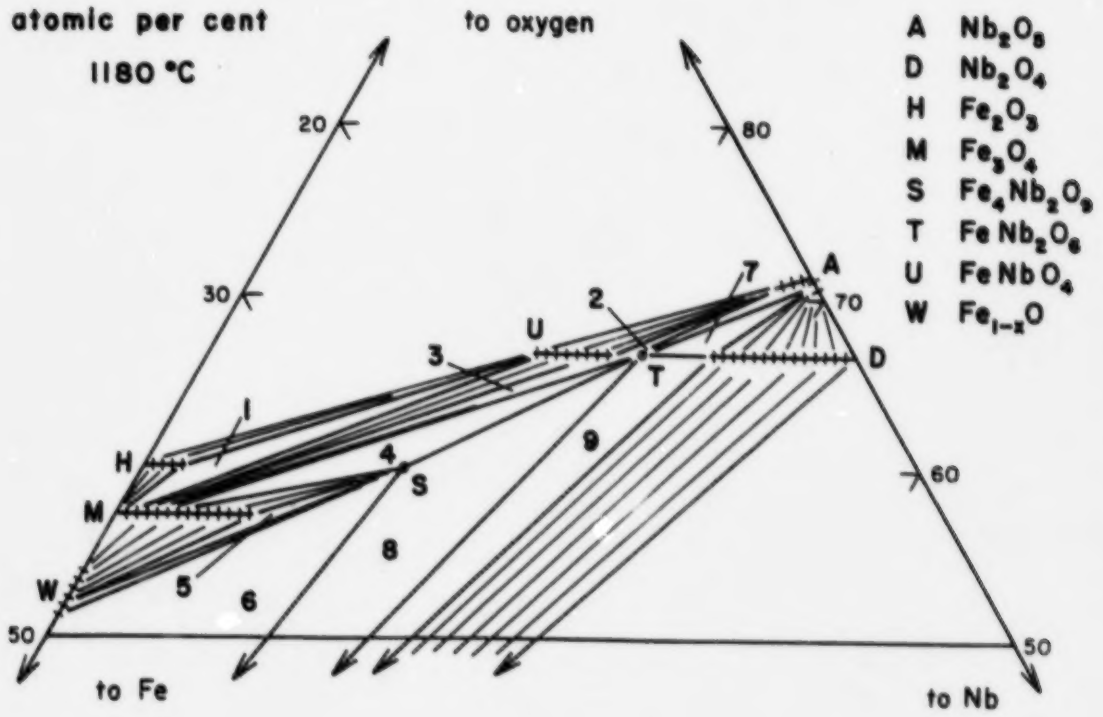

Figure 2. Isothermal, polybaric section of a part of the system Fe-Nb-O. Data from Table I. The 3-solid-phase triangles are numbered, and they are listed in Table II with their univariant partial pressures of oxygen. The compositional range of wüstite in the system Fe-O is from Darken and Gurry[20]. Hatched lines represent extent of solid solutions.

(i) α-Nb_2O_5 (designated "A" in Figures 1 and 2 and in Tables I and II). The powder pattern (taken at room temperature) of material heated in air at 1180°C and quenched, corresponds to that described as the monoclinic high-temperature (α) phase[4, 5]. Other lower-temperature polymorphs have been described and have been shown to be metastable[4, 5, 6].

This compound is known to have a range of non-stoichiometry from $NbO_{2.50}$ to $NbO_{2.42}$ [7, 8, 9], and, within this range, discrete phases with Magnéli ordering relationships have been reported[8]. The present work is not sufficiently detailed to relate the stability of the discrete phases to discrete ranges of oxygen pressure. The stoichiometric compound is white; the non-stoichiometric material is blue-black. The colour change takes place at oxygen pressures between $\log f_{O_2} = -9.1$ and -9.9 (1180°C).

The reduction of Phase A, having the minimum oxygen content (assumed to be $NbO_{2.42}$ after Ref. 9) to NbO_2, was found to take place at $-13.2 > \log f_{O_2} > -17$. This corroborates the value of -14.0 interpolated from the data of Coughlin[10].

The oxide Nb_2O_5 will take some ferric iron into solid solution, giving it a dark olive-green colour. The maximum amount at 1180°C, 2 ± 1 at. % Fe, is based on the amount of $FeNbO_4$ (U) that was found with the solid solution (Phase A) after annealing 72 hours at 1180°C at $P_{O_2} = 1$, Fe:Nb = 1:9, bulk composition Fe = 3.0 at. %., O = 70.5%. The amount of Phase U was estimated by observation (polished section) to be between 0.5

and 2 vol.%. The effect of this solid solution on the powder pattern is a displacement of lines in such a way that a broad line in the solid solution pattern takes the place of two or more weaker lines in the Nb_2O_5 pattern. Also, many of the weak lines in the Nb_2O_5 pattern are not visible in the pattern of the solid solution (see Table III). The pattern of the solid solution is similar to that of the intermediate temperature (830 to 1000°C) polymorph, the H-form of Brauer[4], also designated the β or α' form by Holtzberg et al[5]. This form, which grows metastably from the low-temperature polymorph during the transition from low (γ) to high (α), has been interpreted[5] as being a poorly crystallized transition form of the α structure. It appears that some ferric iron impurity stabilizes the α' structure.

(ii) Nb_2O_4 (designated "D"). This black oxide is capable of taking large amounts of $FeNb_2O_6$ (Phase T, see vii below) into solid solution by the substitution:

$$Nb_2^{+4}O_4 \longleftrightarrow Fe_{0.67}^{+2}Nb_{1.33}^{+5}O_4$$

The maximum amount of substitution produced by synthesis was found by interpolation in Figure 1 to be at Fe = 9.1 $\pm$ 0.6 at. %, which is equivalent to $Fe_{0.54}Nb_{1.46}O_4$ or 81 mol. % T.

This substitution of cations raises the activity of oxygen so that there is an increase in the isothermal f_{O_2} of oxidation. This is illustrated in Figure 1.

The crystal structure of Nb_2O_4 has been described[11] as a supercell of a sub-lattice of the rutile type. However, the powder patterns of the solid solutions do not have the weak lines of the supercell, indicating that the substitution stabilizes the rutile structure. The distorted (Nb_2O_4) and undistorted (solid solution) structures are compared by their powder diagrams in Table IV.

(iii) Fe. Metallic iron was identified by its powder pattern as a phase in assemblages produced by reduction at relatively low oxygen pressures. The low-temperature polymorph (α) was observed, which suggests that the quenching procedure was not fast enough to preserve the high-temperature (γ) structure. The amount of alloying of Nb was not investigated.

(iv) Fe_2O_3 (designated "H"). Hematite can incorporate a small amount of Nb into solid solution; the weight changes observed indicate that the substitution is

$$3\,(Fe_2^{+3}O_3) \longleftrightarrow Fe_4^{+2}Nb_2^{+5}O_9 \text{ (S, see vi below)}$$

The maximum amount, found by interpolation in Figure 1, is 2.0 ± 1.0 at.% Nb, which is $Fe_{5.7}Nb_{0.3}O_9$ or 15 mol. % S.

(v) Fe_3O_4 (designated "M"). Magnetite can incorporate considerable amounts of niobium by the substitution

$$3\,(Fe_3O_4) \longleftrightarrow Fe_7^{+2}Nb_2^{+5}O_{12}$$

The maximum amount, found by interpolation in Figure 1, is 7.6 ± 1.0 at.% Nb, which is $Fe_{7.41}Nb_{1.59}O_{12}$ or 80 mol. % $Fe_7Nb_2O_{12}$.

Although the principal substitution, as described above, maintains the stoichiometric ratio of cations:oxygens of spinels, there is also a small amount of cation-excess non-stoichiometry. Large amounts had been found in the tantalian magnetites[3]. Niobian magnetites were equilibrated with various oxygen pressures within the stability range of the particular composition under study, and some changes in their composition were indicated by changes of the magnetic properties (see below). However, corresponding weight changes were not observed, so that the amount of variation in oxygen content is within the limits of detection, 0.3 at. % oxygen.

The expansion of the spinel structure by this substitution is shown in Figure 3 (data in Table V). It is similar and comparable to that of the analogous substitution in the system Fe-Ta-O,[3] for which the data have been included in Figure 3 for comparison.

The effect of the substitution on the magnetic permeability was tested by placing the samples in the core of a small coil and measuring the relative changes of inductance produced. Such measurements are inversely proportional to the permeability; however, the relationship is complicated by differences in grain size and packing. The permeability ratios, listed in Table V, show a decrease in the permeability corresponding to an increase in the amount of substitution.

The composition of this phase will change in response to variations of oxygen pressure, as shown in Figure 4. If a solid solution is subjected to an oxygen pressure greater than that of the upper (oxidation)

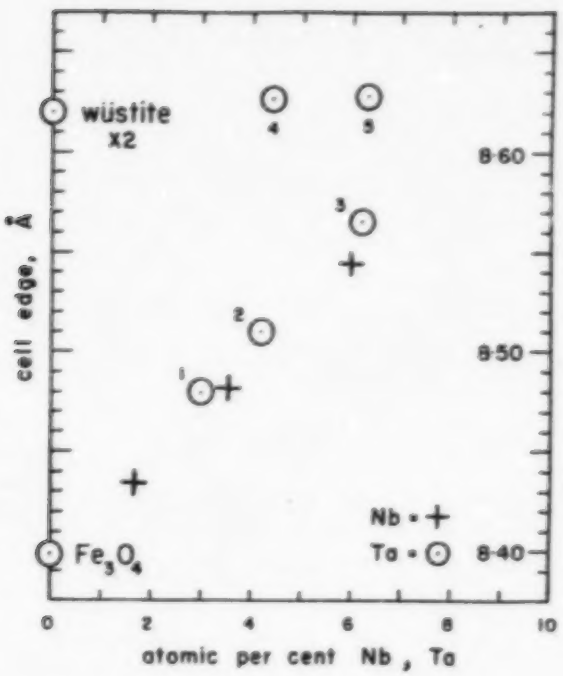

Figure 3. Cell dimensions of niobian magnetites, data from Table V. Dimensions of wüstite and tantalian magnetites[3] are for comparison; of these, only Numbers 1, 2 and 3 are stoichiometric spinels, Numbers 4 and 5 are cation-excess spinels.

boundary curve for any given composition, then oxidation will proceed in such a way that the composition of the solid solution will change by moving along the upper boundary curve toward Fe_3O_4, reaching, at equilibrium, the composition where the curve is intersected by the given oxygen pressure. Also, another phase, higher in Nb:Fe ratio than the original composition, will be exsolved. The exsolved phase will be S ($Fe_4Nb_2O_9$) in the range of log f_{O_2} from -10.5 ± 0.7 to -8.1 ± 1.0, it will be the compound T ($FeNb_2O_6$ with some $FeNbO_4$ in solid solution) in the range -8.1 ± 1.0 to -5.6 ± 1.6, and will be the phase U ($FeNbO_4$ with some $FeNb_2O_6$ in solid solution) in an undetermined range that is included within the uncertainty of -5.6 ± 1.6. Oxygen pressures in excess of log $f_{O_2} = -5.6 \pm 1.6$ will produce the assemblage H (Fe_2O_3) + U. The reduction of a magnetite solid solution will take place at oxygen pressures lower than that given by the lower (reduction) boundary curve in Figure 4. The reaction occurring will be a change in composition to the right along the boundary curve, plus the exsolution of wüstite. At oxygen pressures lower than log $f_{O_2} = -11.2$, magnetite solid solution will decompose to wüstite plus phase S ($Fe_4Nb_2O_9$).

(vi) $Fe_4Nb_2O_9$ (designated "S"). This phase has been previously synthesized and described by Bertaut et al.[12].

The stability of this phase in terms of variable oxygen pressure is limited by the reactions that form the univariant assemblages 4 and 5 in Figure 2 and Table II.

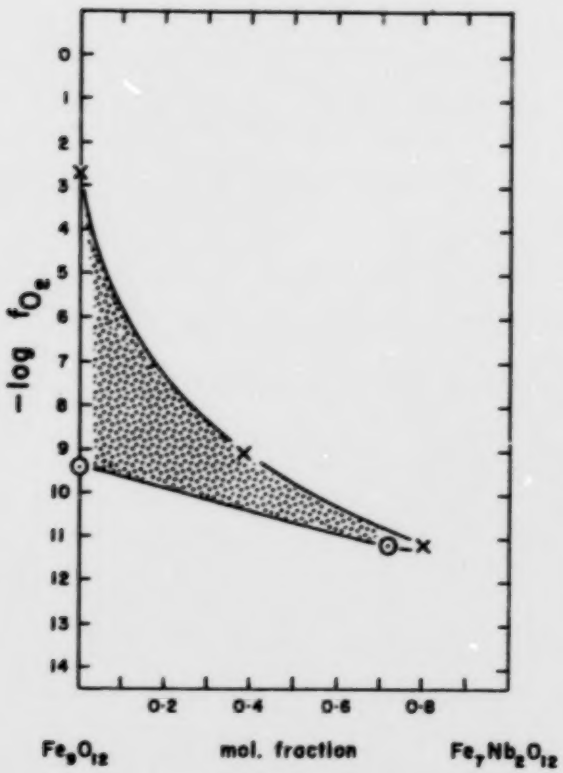

Figure 4. The oxygen pressure vs. composition stability field of niobian magnetites at 1180°C.

(vii) $FeNb_2O_6$ (designated "T"). This brown oxide has the orthorhombic structure[13] of the columbite mineral series, of which it is an end-member. Crystallographically, it is related to wolframite. The unit cell is a super-cell, tripled along z, of a subcell of the o'rh.-wolframite type[14, 15].

This phase may incorporate small amounts of $FeNbO_4$ (Phase U) by the substitution:

$$Fe^{+2}_{0.67}Nb^{+5}_{1.33}O_4 \longleftrightarrow Fe^{+3}Nb^{+5}O_4$$

The maximum amount of this substitution at 1180°C is reported to be 15 ± 5 mol. % $FeNbO_4$[16].

The positions of the tie-lines (Figure 1) indicate that the amount of solid solubility with Phase D (see (ii) above) is less than 1 mol. % Nb_2O_4.

(viii) $FeNbO_4$ (designated "U"). This dark brown oxide can be synthesized easily in air[17, 18]. Three polymorphs have been described[15,19], viz. (1) monoclinic (wolframite-type, with ordered cation distribution) stable between 25 and 1085°C, (2) orthorhombic (ortho. wolframite type, with random cation distribution) 1085 to 1380°C, and (3) tetragonal (rutile-type) 1380 to 1410°C (melting). In the present work, the synthesis of the ortho. wolframite type is in accord with the previous studies.

Large amounts of $FeNb_2O_6$ may be incorporated in solid solution, by the equation noted in (vii) above. Phase T is not exactly isomorphous with phase U, but the structures are very similar, both being wolframite types, and the difference being in the ordering of the cations in

Phase T to form a tripled supercell[2]. The maximum amount of this substitution at 1180°C is reported to be at 65 ± 5 mol. % T[16].

This substitution increases the ratio Fe^{+2}:Fe^{+3}; the solid solutions, therefore, have smaller equilibrium vapor pressures of oxygen. The behaviour of these solid solutions, when subjected to variable oxygen pressure, will be similar to that described for the analogous tantalian compounds[3].

The mineral ixiolite, which has the orthorhombic wolframite structure, is $(Ta, Fe, Sn, Nb, Mn)_4O_8$[2]. This composition has several AO_2 and ABO_4 end-members, of which $FeNbO_4$ is one.

CONCLUSIONS

It can be seen in Figure 2 that the ternary solid solutions of Phases M, H, R and D have invariable cations:oxygens ratios. The substitution of cations takes place with the maintenance of numbers in spite of variation in their charges from +2 to +5. The charge balance is maintained by pairing low-valence cations with high-valence cations.

The structures of these phases all have the oxygen atoms in a close-packed arrangement. The oxygen frameworks maintain their stability when accommodating cations of different charges and sizes (1) by distortion of the framework, usually with resultant change of symmetry, or (2) by ordering of the cations to produce a supercell (i.e., $FeNb_2O_6$).

ACKNOWLEDGEMENTS

Valuable suggestions were received from Drs. N.F.H. Bright, A.H. Webster and Mr. J.F. Rowland. Technical help was received from the staff of the Physical Chemistry Section. Mr. G.E. Alexander of the Mineral Physics Section made permeability measurements on the magnetites.

ACT:ST

TABLE I

Reactions Observed at T = 1180°C and Various Oxygen Pressures

The reactions, as listed, show only the solid phases involved, omitting vapor. In order to balance these equations, O_2 must be added where appropriate. In any assemblage, the phases are listed in order of abundance. Abbreviations: f_{O_2} = oxygen pressure, A = α-Nb_2O_5, D = Nb_2O_4, H = Fe_2O_3, M = Fe_3O_4, S = $Fe_4Nb_2O_9$, T = $FeNb_2O_6$, U = $FeNbO_4$, W = $Fe_{1-x}O$. The letter abbreviations also include solid solutions. Total pressure 1 atm.

f_{O_2} (atm.) gas mixture	Fe:Nb (atoms)	Time (hours)	Reaction (solids only)	Change in atomic % oxygen in solids
10^{-17}	0:1	25	A → D + A	71.4 → 68.1
	1:9	8	A + U → D	70.6 → 66.8
CO	1:4	6	D → D	66.7 → 66.7
	3:7	16	T + A → T + D	67.0 → 66.7
	2:3	8	U + A → T + Fe	67.7 → 63.8
$10^{-13.2}$	0:1	23	A → A	71.3 → 71.3
	1:9	8	A → D	70.6 → 67.2
	1:4	6	D → D	66.7 → 66.7
$\frac{CO}{CO_2}=\frac{10}{1}$	1:3	8	D → D	66.7 → 66.7
	3:7	32	T + D + A → T + D	66.9 → 66.7
	1:2	8	T → T	66.7 → 66.6
	2:3	8	T + Fe → T + Fe	63.8 → 64.1
	3:2	15	H + U → T + Fe	65.5 → 54.8
$10^{-12.6}$	0:1	5	A → A	71.4 → 71.3
	1:9	8	D → A + D	66.7 → 69.4
	1:9	7	A + U → A + D	70.6 → 69.7
	1:4	8	D → D + A	66.7 → 67.7
$\frac{CO}{CO_2}=\frac{5}{1}$	1:3	15	D → D	66.7 → 66.8

Table I continued

f_{O_2} gas mixture	Fe:Nb	Time (hours)	Reaction (solids only)	Change in atomic % oxygen in solids
	3:7	9	T + D + A → T + D	67.0 → 66.8
	3:2	7	H + U → S + T + Fe	65.5 → 59.3
	3:2	8	S + T + Fe → T + Fe	59.3 → 54.8
	3:1	30	S + Fe → Fe + T	53.0 → 42.9
$10^{-12.2}$	0:1	8	A → A	71.4 → 71.1
	1:9	8	A + D → A + T	69.7 → 70.0
	1:4	8	D → D + A	66.7 → 68.1
	1:3	15	D → T + A	66.7 → 68.0
	3:7	24	T + D → T + A	66.7 → 67.2
$\frac{CO}{CO_2} = \frac{3}{1}$	1:2	7	T → T	66.7 → 66.7
	1:1	7	U → S + T	66.7 → 63.5
	3:1	12	U + H → S + W + Fe	63.6 → 56.5
	3:1	9	S + W + Fe → S + Fe + W	56.5 → 55.9
	4:1	8	H + U → S + W + Fe	62.9 → 54.9
	24:1	12	Fe + S → Fe + S	15.3 → 15.3
$10^{-11.8}$	3:1	8	U + H → S + W	63.6 → 57.9
$\frac{CO}{CO_2} = \frac{2}{1}$				
$10^{-11.2}$	0:1	8	A → A	71.4 → 71.3
	1:4	8	D → T + A	66.7 → 68.6
$\frac{CO}{CO_2} = \frac{1}{1}$	3:2	8	U + H → S + T	65.5 → 61.3
	3:1	42	H + U → S + W	63.6 → 58.0
	4:1	8	H + U → M + S	62.9 → 57.5
	4:1	147	M + S → S + W	57.5 → 56.5
	6:1	8	H + U → S + W + T	62.2 → 55.9
	6:1	10	S + W + T → S + W	55.9 → 54.6
	11:1	23	H + U → S + W + M	61.3 → 54.0
$10^{-9.8}$	0:1	24	A → A	71.3 → 71.3
$\frac{CO}{CO_2} = \frac{1}{5}$	4:1	7	H + U → M + S	62.9 → 58.2
	6:1	8	H + U → M	62.2 → 57.3
	11:1	7	H + U → M + W	61.3 → 55.9
	24:1	7	H + U → M + W	60.6 → 56.5

Table I continued

f_{O_2} gas mixture	Fe:Nb	Time (hours)	Reaction (solids only)	Change in atomic % oxygen in solids
$10^{-9.4}$ $\frac{CO}{CO_2}\frac{1}{8}$	11:1	6	M ⟶ M	57.1 ⟶ 57.0
$10^{-9.1}$ $\frac{CO}{CO_2}\frac{1}{12}$	0:1	12	$A_{bl.}$ ⟶ $A_{wh.}$	71.3 ⟶ 71.3
	1:9	8	A + U ⟶ A + T	70.6 ⟶ 70.1
	1:2	7	T ⟶ T	66.7 ⟶ 66.8
	2:3	24	U + A ⟶ T + S	67.7 ⟶ 65.7
	1:1	6	U ⟶ T + S	66.7 ⟶ 63.6
	3:2	8	U + H ⟶ S + T	65.5 ⟶ 62.0
	3:1	24	U + H ⟶ S + M	63.6 ⟶ 59.4
	4:1	8	H + U ⟶ M + S	62.9 ⟶ 58.6
	6:1	31	H + U ⟶ M + S	62.2 ⟶ 58.1
	11:1	8	H + U ⟶ M	61.3 ⟶ 57.2
	24:1	8	H + U ⟶ M	60.6 ⟶ 57.1
	1:0	8	H ⟶ M	60.0 ⟶ 57.1
$10^{-7.2}$ $\frac{CO}{CO_2}\frac{1}{100}$	1:2	96	T ⟶ T	66.8 ⟶ 66.9
	2:3	63	U + A ⟶ T + M	67.7 ⟶ 66.0
	1:1	62	U ⟶ T + M	66.7 ⟶ 64.8
	3:2	86	U + H ⟶ T + M	65.5 ⟶ 63.3
	6:1	157	M ⟶ M + T	57.1 ⟶ 59.0
	11:1	48	H + U ⟶ M + T	60.9 ⟶ 58.8
	24:1	39	H + U ⟶ H + U	60.6 ⟶ 60.1
$10^{-4.0}$ CO_2 (purified)	1:2	8	T ⟶ U + A	66.8 ⟶ 68.2
	2:3	48	U + A ⟶ U + A	67.7 ⟶ 67.0
	1:1	64	S + T ⟶ U	63.6 ⟶ 66.5
	3:2	7	U + H ⟶ U + H	65.5 ⟶ 65.4
	3:1	4	U + H ⟶ U + H	63.6 ⟶ 63.4
	6:1	38	H + U ⟶ H + U	62.2 ⟶ 61.9
	11:1	39	H + U ⟶ H + U	61.3 ⟶ 60.5
	24:1	15	H + U ⟶ H	60.6 ⟶ 60.1
0.21 air	0:1	2	A ⟶ A	71.4 ⟶ 71.4
	1:4	11	D ⟶ A + U	66.7 ⟶ 69.7
	6:1	8	H + U ⟶ H + U	62.2 ⟶ 62.1
	11:1	14	H + U ⟶ H + U	61.3 ⟶ 61.2
	24:1	6	H + U ⟶ H + U	60.6 ⟶ 60.5

Table I continued

f_{O_2} gas mixture	Fe:Nb	Time (hours)	Reaction (solids only)	Change in atomic % oxygen in solids
1.0 O_2	1:9	80	A + U ⟶ A + U	70.6 ⟶ 70.6
	1:3	15	D ⟶ U + A	66.7 ⟶ 69.3
	1:2	4	T ⟶ U + A	66.8 ⟶ 68.3
	1:1	7	U ⟶ U	66.7 ⟶ 66.7
	3:1	4	H + U ⟶ H + U	63.6 ⟶ 63.6

TABLE II

Univariant Assemblages at 1180°C

Numbered as in Figure 2. Abbreviations as in Table I and Figure 2.

Assemblage	log f_{O_2} at 1180°C
1. H + U + M + V (vapour)	-5.6 ± 1.6
2. U + A + T + V	-5.6 ± 1.6
3. U + M + T + V	-5.6 ± 1.6
4. S + M + T + V	-8.1 ± 1.0
5. S + M + W + V	-10.5 ± 0.7
6. S + W + Fe + V	-11.7 ± 0.5
7. T + A + D + V	-12.4 ± 0.2
8. S + T + Fe + V	-12.4 ± 0.2
9. T + D + Fe + V	$<-17.$

TABLE III

X-Ray Powder Diffraction Patterns of α-Nb_2O_5 and its Ferrian Solid Solution

Taken at room temperature; camera diameter 57.3 mm; Cobalt K_α, $\lambda = 1.790$ A. Materials fired at 1180°C, quenched to room temperature.

α-Nb_2O_5		Solid Solution Nb_9FeO_{24}	
I	d (A)	I	d (A)
3	5.65	5	7.2
20	5.11	15	5.11
15	4.65	15	4.73
60	3.72	30	3.71
90	3.63	30	3.70
100	3.47	100	3.57
10	3.35	30b	3.40
30	2.83	10	3.32
15	2.77	30	2.77
20	2.70		
15	2.54	2	2.50
5	2.49		
10	2.31	10	2.30
2	2.10	2	2.10
5	2.08	10	2.05
8	2.04	10	2.04
15	1.909	15	1.905
2	1.853		
5	1.818	8	1.785
10	1.742		
5	1.709	5	1.702
20	1.684	20b	1.680
10	1.678	10	1.668
8	1.589		
10	1.580	15	1.576
5	1.554	2	1.552
5	1.525		
2	1.453	3	1.453

TABLE IV

X-Ray Diffraction Powder Patterns of Nb_2O_4 and its Ternary Solid Solutions

Taken at room temperature; camera diameter 57.3 mm; Cobalt K_α, $\lambda = 1.790$ A. Materials fired at 1180°C, quenched to room temperature.

Nb_2O_4		Solid Solution $Nb^{+4}Nb_2^{+5}Fe^{+2}O_8$	
I	d (A)	I	d (A)
2	3.76		
2	3.62		
80	3.41	100	3.37
3	3.18		
100	2.54	90	2.56
25	2.41	20	2.38
15	2.24	10	2.26
1	2.15	2	2.137
2	1.977		
2	1.929		
5	1.893		
3	1.854		
5	1.789		
100	1.747	100	1.747
30	1.705	30	1.681
15	1.525	10	1.520
10	1.495	20	1.507
40	1.418	40	1.406
30	1.369	30	1.392

TABLE V

Cell Dimensions and Permeability Ratios of Niobian Magnetites

Material synthesized at 1180°C. X-ray powder diffraction at room temperature, using as an internal standard the (220) (α_1) line of MgO at $2\theta = 73.842°$. Cobalt $K\alpha_1$ $\lambda = 1.7889$ A.

Experiment no.	Composition	$\underline{a}$ (A)	Permeability Ratio
J	Fe_3O_4	8.398 ± 0.002	1.45
9-11	$Fe_{8.63}Nb_{0.36}O_{12}$		1.31
9-2	$Fe_{8.63}Nb_{0.36}O_{12}$	8.436 ± 0.001	1.23
10-8	$Fe_{8.26}Nb_{0.75}O_{12}$		1.22
10-4	$Fe_{8.26}Nb_{0.75}O_{12}$	8.482 ± 0.001	
8-7	$Fe_{7.71}Nb_{1.26}O_{12}$	8.545 ± 0.001	1.16
	Air		1.00

REFERENCES

1. E.H. Nickel, J.F. Rowland and R.C. McAdam, "Wodginite-a new tin manganese tantalate from Wodgina, Australia, and Bernic Lake, Manitoba," Can. Min., 7 [3] 390-402 (1963).

2. _____, _____ and _____, "Ixiolite-a columbite substructure," Am. Min., 48 [9] 961-79 (1964).

3. A.C. Turnock, "Fe-Ta-Oxides:Phase Relationships at 1200°C. Mineral Sciences Div. Report MS-64-45 (1964). J. Am. Ceram. Soc., 48 [5] (in the press) (1965).

4. G. Brauer, "Die Oxyde des Niobs," Zeit. anorg. Chemie, 248, 1-31 (1941).

5. F. Holtzberg, A. Reisman, M. Berry and M. Berkenblit, "The Polymorphism of Nb_2O_5," J. Am. Chem. Soc., 79, 2039-43 (1957).

6. H.J. Goldschmidt, " A High-temperature X-ray study of Nb_2O_5," J. Inst. Metals, 87, 235-9 (1959).

7. G. Brauer, "Über das magnetische Verhalten der Nioboxyde," Zeit. anorg. Chemie, 256, 10-14 (1948).

8. R. Norin and A. Magneli, "Neue diskrete Nioboxydphasen," Naturwiss., 47, 354-5 (1960).

9. R. Norin, "The Crystal Structure of $Nb_{12}O_{29}$ (o-rh)," Acta Chem. Scand., 17, 1391-1404 (1963).

10. J.P. Coughlin, "Theoretical Metallurgy: XII, Heats and Free Energies of Formation of Inorganic Oxides," U.S. Bureau of Mines Bull., 542 (1954).

11. B-O. Marinder, "The Crystal Structure of NbO_2, " Arkiv Kemi, 19 [30] 435-46 (1962).

12. F. Bertaut, L. Corliss, F. Forrat, R. Aleonard and R. Panthenet, "Étude de Niobates et Tantalates de Métaux de Transition Bivalents," Phys. Chem. Solids, 21 [3] 234-51 (1961).

13. J.H. Sturdivant, "The Crystal Structure of Columbite," Zeit. Krist., Abt. A 75,88-108 (1930).

14. H. Schröcke, "Heterotype Mischbarkeit zwischen Wolframit-und Columbitgruppe," Beitr. Min. Petrog., 8, 92-110 (1961).

15. F. Laves, G. Bayer and A. Panagos, "Strukturelle Beziehungen zwischen den Typen der α-PbO_2, $FeWO_4$ (Wolframit) und $FeNb_2O_6$ (Columbit), und über die Polymorphie des $FeNbO_4$," Schweiz. Min. Petr. Mitt., 43 [1] 217-34 (1963).

16. H. Schröcke, Personal communication, 1964.

17. K. Brandt, "X-ray studies on ABO_4 compounds of Rutile Type and AB_2O_6 compounds of Columbite Type," Arkiv Kemi, Min. Geol., 17, No. 15 (1943).

18. H. Schröcke, "Heterotype Mischbarkeit zwischen Wolframit-und Rutilgruppe," Beitr. Min. Petrog., 8, 339-48 (1962).

19. R.S. Roth and J.L. Waring, "Ixiolite and other polymorphic types of $FeNbO_4$," Am. Min., 49, 242-5 (1964).

20. L.S. Darken and R.W. Gurry, "The System Iron-Oxygen: II, Equilibrium and Thermodynamics of Liquid Oxide and Other Phases," J. Am. Chem. Soc.,68 [5] 798-816 (1946).

- - - -